ENGINEERING TRANSACTIONS • Engng. Trans. • 45, 2, 181–198, 1997
Polish Academy of Sciences • Institute of Fundamental Technological Research

INFLUENCE OF RECOVERY ON PLASTIC ANISOTROPY OF METALS

G. SOCHA (WARSZAWA)

The paper describes experimental investigations of plastic anisotropy changes during recovery of plastically deformed metals. Two materials differing in crystallographic structure and manufacturing processes were investigated by means of uniaxial tests: aluminium alloy PA6 and mild steel denoted as 45 according to Polish Standards. Additionally, changes of the strain of previously deformed and unloaded material and the influence of the dynamic recovery on the shape of stress-strain curve for cyclic loading of the material were investigated. All tests were performed at room temperature. The first experiment showed that plastic anisotropy of deformed and then unloaded material begins to change immediately after plastic deformation. The changes of anisotropy parameters k, α_x and Δk were shown as the functions of recovery time. Additionally, the changes of plastic anisotropy were shown in the form of cross-section of the yield surface with the plane $\sigma_x - \tau_{xy}$ in the stress space. The second experiment showed that the strain of uniformly plastically deformed and unloaded material changes after unloading. The last experiment showed that the shape of the stress-strain curve is influenced by dynamic recovery of the material.

1. INTRODUCTION

It is now believed that the shape of the stress-strain curve is the result of dynamic balance between strain-hardening and recovery [3]. This balance is achieved after introduction of plastic deformation into the material. Investigations presented in this paper have been concentrated on determining the changes of the form of the stress-strain curve for different paths of subsequent loadings. These changes can also affect the state of plastic anisotropy (that can be observed as the variation of the Bauschinger effect).

The state of plastic anisotropy is a very important technological parameter. For example, drawability of metal sheets is related to the value of the normal anisotropy coefficient. If we assume, that the state of plastic anisotropy varies in time after deformation (so does the normal anisotropy coefficient), it is possible that the drawability of cold-worked metal sheets may also undergo some changes. This effect was observed in mild steel sheets: the recovery proceeds at a slow but observable rate during storage of such sheets at the room temperature, and the sheet needs temper rolling before being used in deep-drawing operations to avoid stretcher strain formation.

Additionally two questions arose during the investigations. The first was whether the recovery of unloaded material affects its strain state. If this were true, the minimisation of such effect would improve the shape stability of cold-worked elements. The second question regards the dynamic (i.e. during loading or unloading) balance between strain-hardening and recovery. If such effects exist, the shape of stress-strain curves for cyclically loaded material should be influenced by loading (or strain) rate. Till now, it was believed that strain rate does not affect the shape of the stress-strain loop in materials during cyclic loading. Answers to these questions may be very important. It is hoped that the results of the investigations presented will furnish the necessary information allowing for the assessment of constitutive models which are used, for example, in FEM computations.

2. Plastic anisotropy

Both materials under investigation were considered to be initially isotropic since the yield stress in tension and compression was proved to be of the same absolute value. The yield condition of virgin material was assumed to be of the Huber-Mises type [1, 2]

$$(\sigma_x - \sigma_y)^2 + (\sigma_y - \sigma_z)^2 + (\sigma_z - \sigma_x)^2 + 6(\tau_{xy}^2 + \tau_{yz}^2 + \tau_{zx}^2) = 6k_0^2 . \tag{2.1}$$

For the plane stress state this yield condition is represented by an ellipsoid shown in Fig. 1. Points Y_x and Z_x correspond to the yield limit in tension and compression, respectively [4, 5]. In Fig. 2 the yield condition for virgin, isotropic material

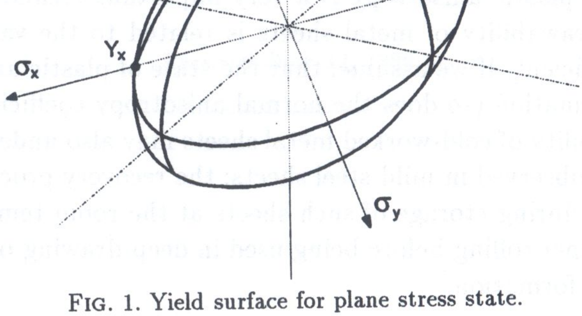

FIG. 1. Yield surface for plane stress state.

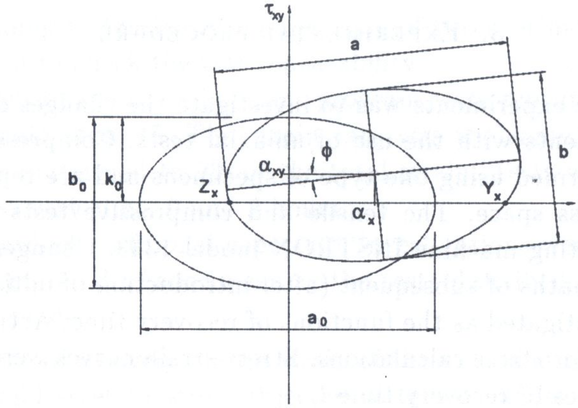

FIG. 2. Anisotropy parameters.

is shown in the plane of non-vanishing stress components σ_x, τ_{xy}, together with a curve corresponding to the yield condition of plastically deformed material. A set of anisotropy parameters can be introduced [6, 7] to describe anisotropy of the strain-hardened material:

- actual lengths a, b of ellipse axes,
- components of ellipse displacement α_x, α_{xy},
- angle of ellipse rotation ϕ.

If initial deformation has been introduced into the material by simple tension ($\alpha_{xy} = 0$ and $\phi = 0$) then, assuming mixed isotropic-kinematic strain-hardening model we can determine a and α_x using uniaxial tests. For an initially isotropic material

$$k_0 = \frac{b_0}{2} = \frac{a_0}{2\sqrt{3}}, \tag{2.2}$$

where k_0 stands for the yield stress in shear. During deformation the a/b ratio remains constant. For uniaxial plastic stress states we can write

$$\sigma_x - \alpha_x = \pm\sqrt{3}k. \tag{2.3}$$

If Y_x stands for the yield stress in tension and Z_x stands for the absolute value of the yield stress under compression, we can determine the anisotropy coefficients as

$$\alpha_x = \frac{Y_x - Z_x}{2}, \qquad k = \frac{Y_x + Z_x}{2\sqrt{3}}. \tag{2.4}$$

These coefficients will be used in the analysis of the test results.

3. Experimental procedure

The aim of the experiments was to investigate the changes of certain plastic anisotropy coefficients with the use of uniaxial tests. Compression and tension tests can be performed using one type of specimens and are represented by two paths in the stress space. The tensile and compressive tests were conducted on closed-loop testing machine INSTRON model 1343. Changes of stress-strain relations for two paths of subsequent (after introduction of initial plastic strain) loading were investigated as the functions of recovery time. Actual area of cross-section was used for stress calculations. Stress-strain curves were determined for four different values of recovery time t_r.

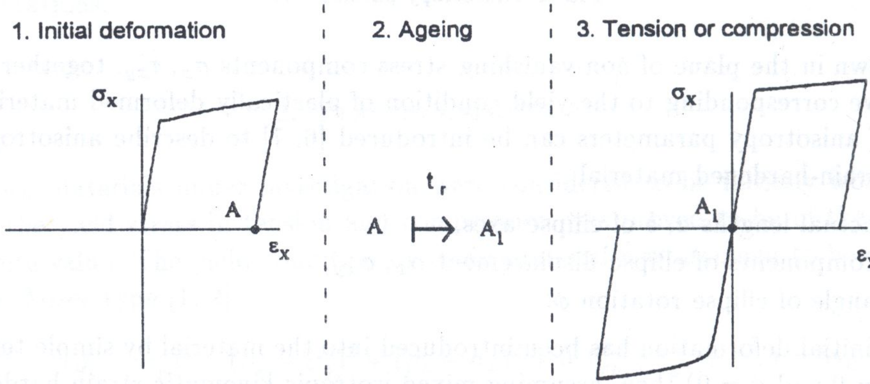

FIG. 3. Test program.

The testing procedure for PA6 aluminium alloy consists of the following stages (Fig. 3):

1. Introduction of initial deformation: four sets, each consisting of four specimens (16 specimens) were extended to 4% of total engineering strain and unloaded (stage 1 in Fig. 3). Tests were strain-controlled with the constant strain rate 0.01%/s for loading and unloading.

2. Ageing: three sets of specimens were then aged at the room temperature during 0.5, 2 and 380 hours, respectively. A set of specimens corresponding to recovery time $t_r = 0$ hours were then subsequently loaded, without stopping the testing machine.

3. Subsequent loading: specimens were subsequently subjected to tension or compression. Each set of specimens corresponding to the same ageing time consisted of four specimens. Two of them were subjected to tension up to 4% of the total strain and the remaining two were compressed to 4% of the total strain (stage 3 in Fig. 3). Tests were strain-controlled with constant rate of 0.01%/s. The ageing time for all four specimens in one set was the same. Two stress-strain

curves corresponding to tension or compression of two specimens from the same set were compared to check the test repeatability.

All three stages of the described test program were repeated with the specimens made of mild steel 45. The strain rate was the same, but compression and tension were performed to 2% of the total strain. Tests were made for two periods of the recovery time: 0 and 2 hours.

The tests regarding additional aspects of investigations were performed with the use of the same kind of specimens as the tests described above. Two additional tests were made:

1. The influence of recovery on the strain of the unloaded material: two specimens made of mild steel 45 were subjected to tension under the strain control with rate 0.01%/s to 2%/s of the total strain, axial strain measurements were continued for 2 hours after unloading.

2. Dynamic recovery during cyclic loading: two specimens made of PA6 aluminium alloy were deformed cyclically with the constant strain rates of 0.0032%/s and 1.6%/s, respectively, the test program consisted of 10 cycles under the strain control, the strain varied from +2% to −2%. The shape of the stress-strain loop was analysed.

4. Experimental details

4.1. Equipment

All tests were performed on servo-hydraulic, closed-loop testing machine under strain control. Axial strain (parameter controlled by the testing machine) was measured by means of a MTS dynamic extensometer, with the measurement range of ±4% on the basis of 25 mm. Additionally, transversal strain was measured by an MTS extensometer specially designed for the diameter measurements. Loading force was measured by an INSTRON load cell of ±100 kN nominal capacity. Data acquisition for all measurement channels was performed by an independent data acquisition system. Acquisition rate was set up to 5 measurements per second for the strain rate of 0.01%/s. About 2000 points were obtained during the loading process. Post-acquisition analysis of data was made with the use of DADiSP software.

4.2. Specimens and material

The specimen shown in Fig. 4 was designed for tension and compression tests and is of the type used in the LCF tests. The materials under investigation were:

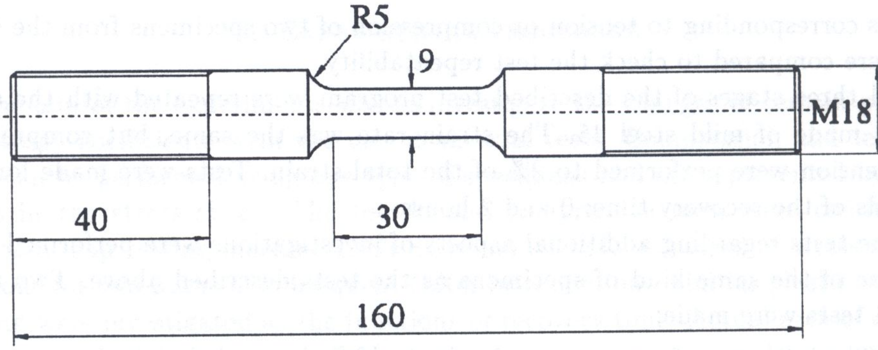

FIG. 4. Specimen.

aluminium alloy PA6 with FCC crystallographic structure and mild steel 45 with BCC crystallographic structure. The chemical composition of PA6 alloy was

$$\{\mathrm{Cu} - 3.8 \div 4.8\%, \quad \mathrm{Mg} - 0.4 \div 1.1\%, \quad \mathrm{Mn} - 0.4 \div 1\%\},$$

and the chemical composition of mild steel 45 was

$$\{\mathrm{C} - 0.42 \div 0.5\%, \quad \mathrm{Mn} - 0.5 \div 0.8\%, \quad \mathrm{Si} - 0.17 \div 0.37\%, \quad P < 0.04\%, \quad S < 0.04\%\}.$$

Specimen made of PA6 aluminium alloy were aged for 2 years at room temperature before the initial deformation.

5. Experimental results

5.1. *Recovery of PA6*

Initial deformation of specimens is shown in Fig. 5. Repeatability of the test due to very accurate machining of the specimens made from a single rod of the material and after ageing of specimens for 2 years is very good. In Fig. 6 subsequent tension of specimens aged for 0, 0.5, 2 and 380 hours, respectively, is shown. For better illustration of the plastic flow of the material, plastic strain only is represented on the horizontal axis. The plastic strain is calculated as a difference between the total measured strain and the quotient of stress and the Young's modulus. Such type of diagram, showing plastic flow of the material, will be used to illustrate subsequent behaviour of aged materials. In Fig. 6 one can see that plastic properties of the material loaded subsequently in the direction of initial loading vary insignificantly, so the influence of recovery can be disregarded.

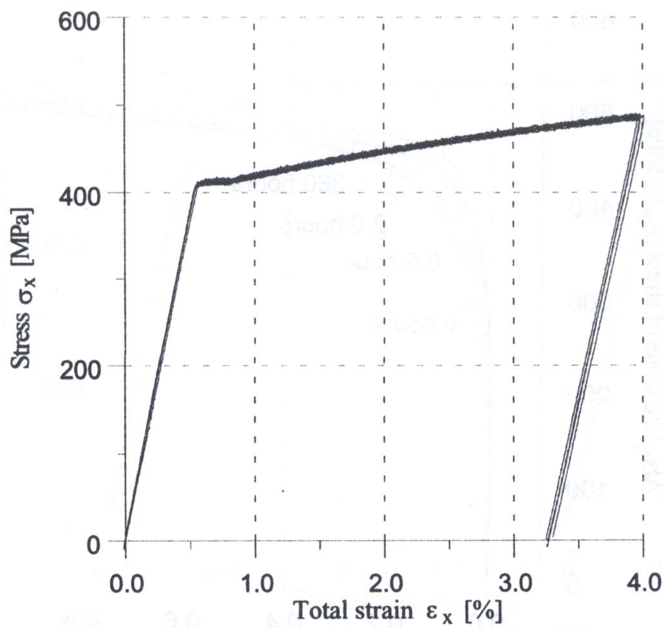

FIG. 5. Initial deformation of specimens made of PA6.

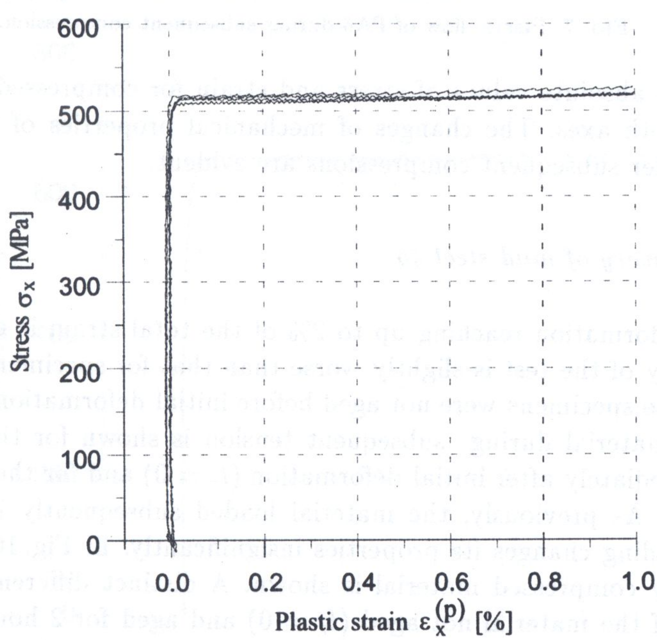

FIG. 6. Plastic flow of PA6 during subsequent tension.

In Fig. 7 plastic flow of the subsequently compressed specimens is shown. For comparison with the plastic flow of subsequently extended specimen (shown by

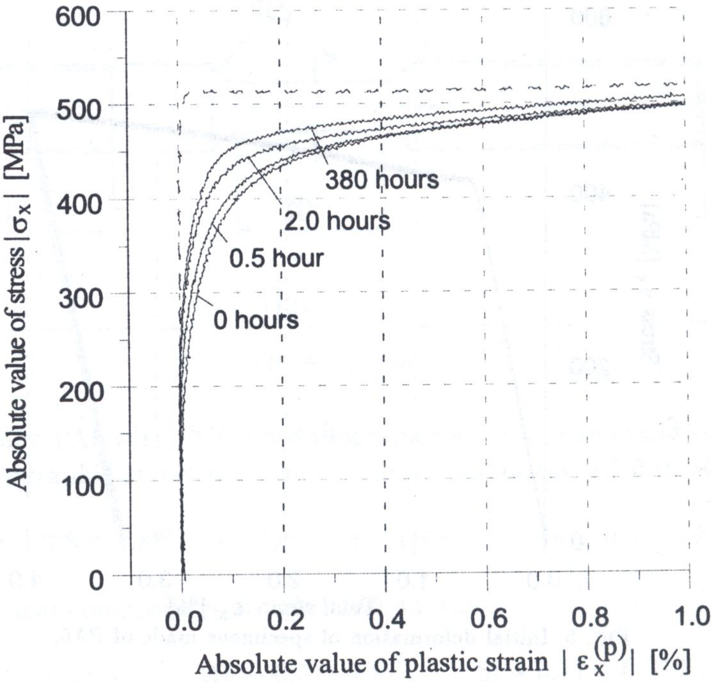

FIG. 7. Plastic flow of PA6 during subsequent compression.

broken line), absolute values of stress and strain for compressed specimens are shown on both axes. The changes of mechanical properties of the prestressed material under subsequent compressions are evident.

5.2. Recovery of mild steel 45

Initial deformation reaching up to 2% of the total strain is shown in Fig. 8. Repeatability of the test is slightly worse than that for specimens made of PA6 alloy, because specimens were not aged before initial deformation. In Fig. 9 plastic flow of material during subsequent tension is shown for the specimen extended immediately after initial deformation ($t_r = 0$) and for the specimen aged for 2 hours. As previously, the material loaded subsequently in the direction of initial loading changes its properties insignificantly. In Fig. 10 plastic flow of subsequently compressed material is shown. A distinct difference between the behaviour of the material not aged ($t_r = 0$) and aged for 2 hours can be seen. For the material instantaneously compressed, unloading is nonlinear and plastic flow begins at point A (for PA6 unloading was linear – see Fig. 5). After 2 hours of ageing, the material can deform linearly – a linear part of stress-strain curve can be observed.

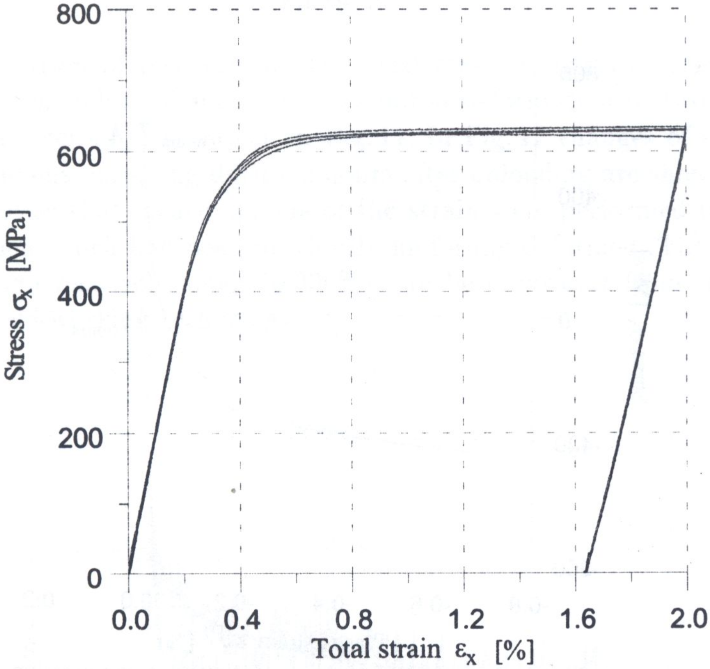

FIG. 8. Initial deformation of specimens made of 45 steel.

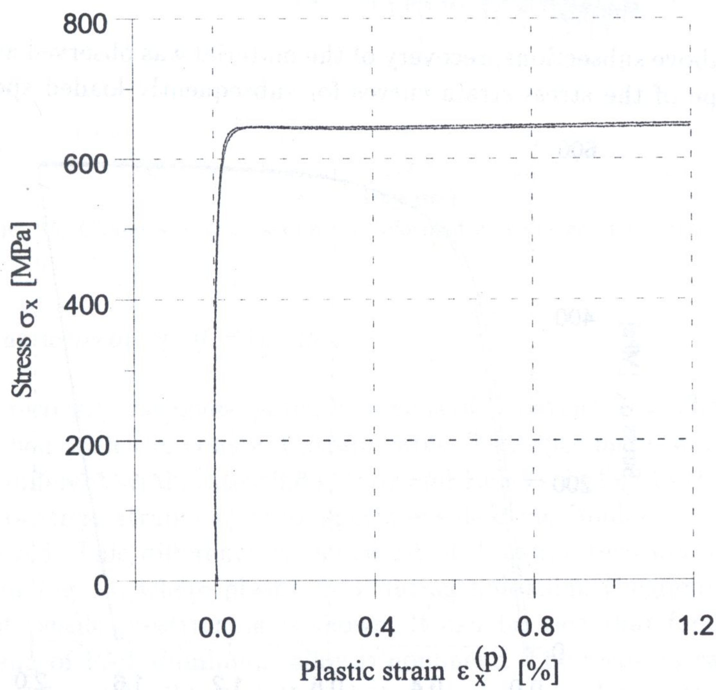

FIG. 9. Plastic flow of 45 steel during subsequent tension.

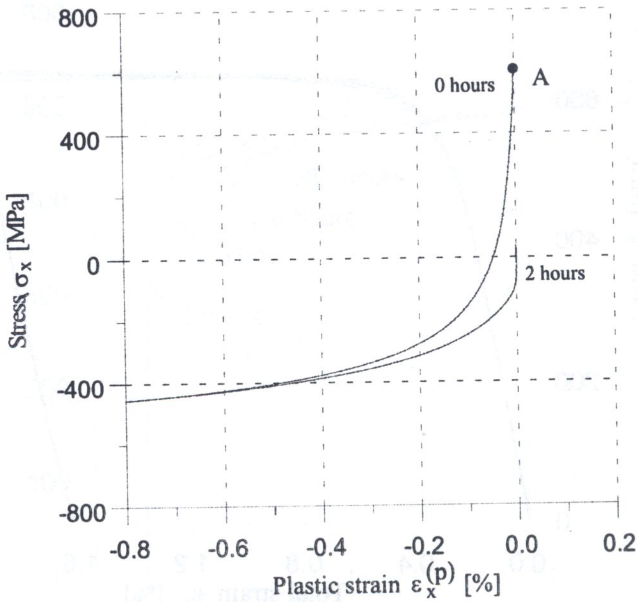

FIG. 10. Plastic flow of 45 steel during subsequent compression.

5.3. *Changes of strain in unloaded mild steel 45*

In the above subsections, recovery of the material was observed as the changes of the shape of the stress-strain curves for subsequently loaded specimens. An-

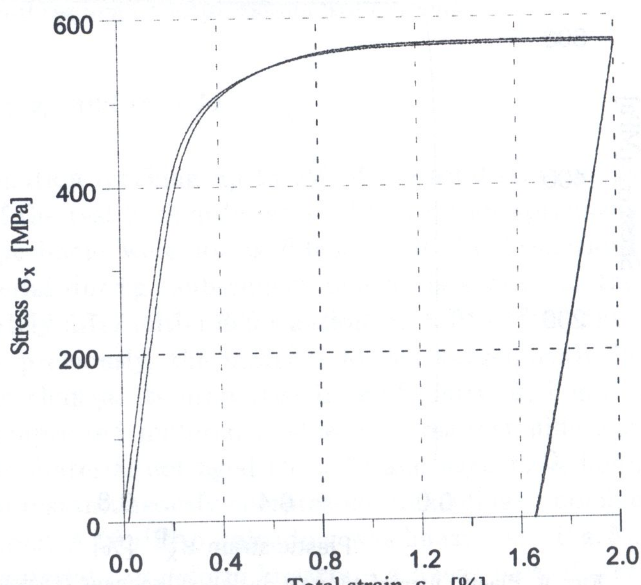

FIG. 11. Initial deformation of specimens made of 45 steel.

other manifestation of recovery are the axial strain changes of plastically deformed and then unloaded material. The initial deformation of two specimens made of mild steel 45 can be seen in Fig. 11. In Fig. 12 changes of axial strain in these specimens occurring during 2 hours after unloading are shown. It is important to notice that measurements of the strain were performed on the part of the specimen which had been previously uniformly deformed. The changes of strain, although relatively small (0.006%), can be important from the point of view of the cold-working technology.

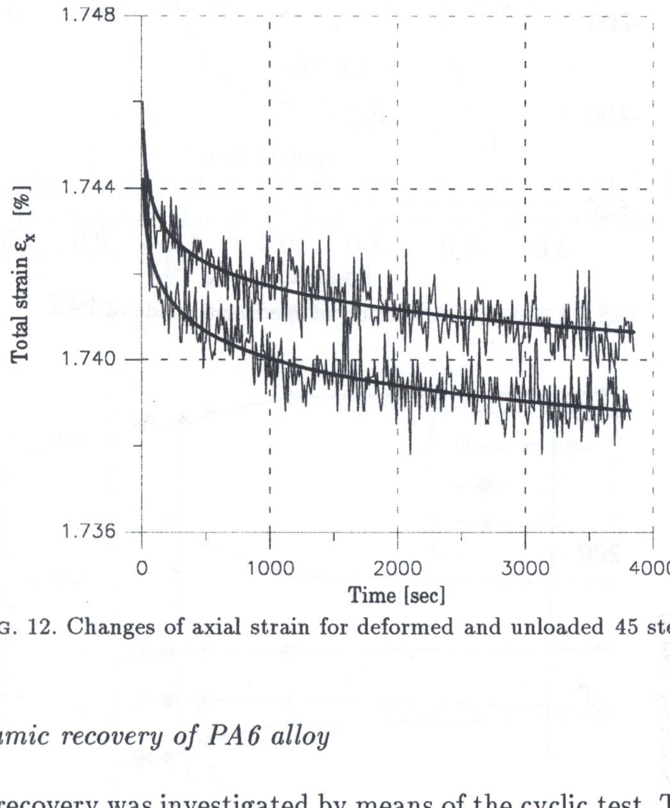

FIG. 12. Changes of axial strain for deformed and unloaded 45 steel.

5.4. *Dynamic recovery of PA6 alloy*

Dynamic recovery was investigated by means of the cyclic test. The tests were strain-controlled with the constant strain rates. Two specimens were tested at significantly different strain rates: 0.0032%/s and 1.6%/s. In Fig. 13 the difference in the shape of stress-strain curves for specimens deformed under two strain rates can be observed. This difference is the result of dynamic recovery, and can be better seen in Fig. 14, where plastic flow during unloading (beginning at point A) after first tensile prestraining is shown. It can be seen that for high strain rate, unloading of PA6 aluminium alloy is nonlinear. The recovery rate for PA6 is higher than that for mild steel 45 and that is why unloading with strain rate 0.01%/s shown in Fig. 5 was linear.

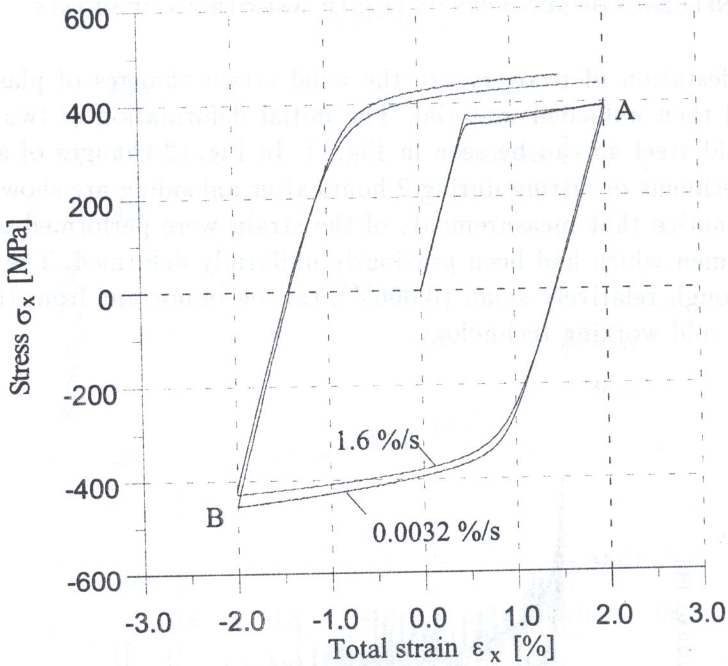

FIG. 13. Cyclic deformation of specimens made of PA6.

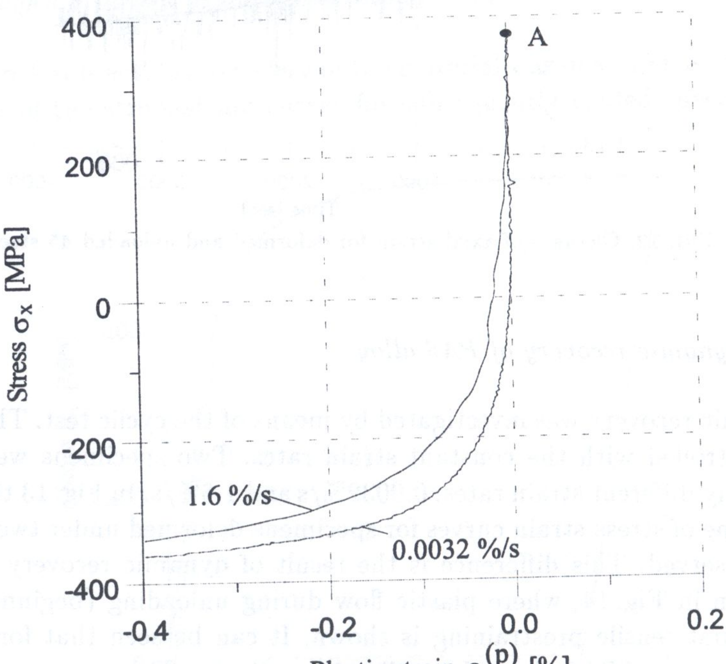

FIG. 14. Plastic flow of PA6 during unloading.

6. Discussion

Changes of anisotropy parameters k and α_x given by (2.4) in time of recovery will be used to illustrate the evolution of plastic anisotropy after introduction of plastic deformation. Additionally, the value of Δk calculated as

$$\Delta k = k - k_0 \tag{6.1}$$

will be shown. The value of k_0 corresponds to yield stress in shear for isotropic material and is shown in Fig. 2. This value is calculated as

$$k_0 = \frac{Y_x^{(i)}}{\sqrt{3}}, \tag{6.2}$$

where $Y_x^{(i)}$ is the yield limit in tension for isotropic material. Yield stress is calculated on the basis of the offset yield point definition for two plastic offsets $\varepsilon_{\text{off}} = 0.01\%$ and $\varepsilon_{\text{off}} = 1\%$.

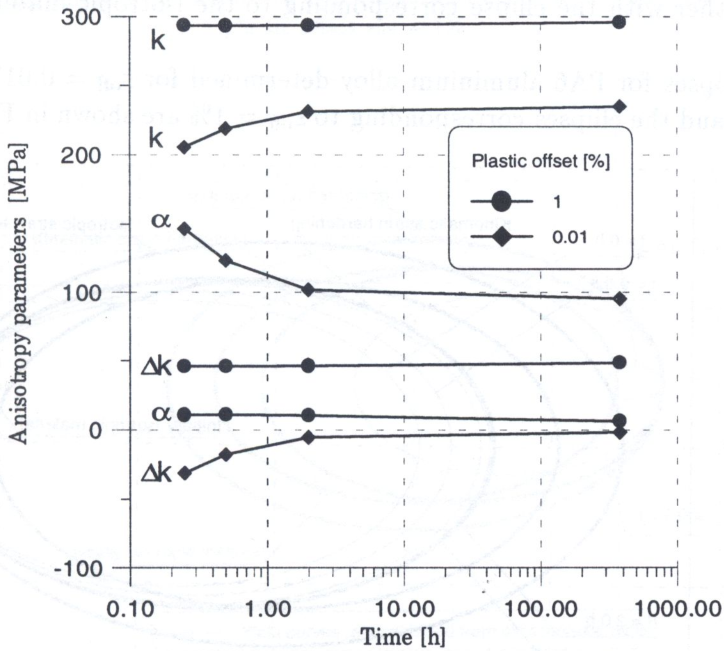

FIG. 15. Evolution of anisotropy parameters during recovery of PA6.

In Fig. 15 changes of anisotropy parameters k, α_x and Δk calculated for two plastic offsets are shown. It can be seen that for $\varepsilon_{\text{off}} = 1\%$, the material behaviour is close to that predicted by isotropic strain-hardening model and the material remains isotropic after deformation – plastic anisotropy and its changes are insignificant. For a small yield offset $\varepsilon_{\text{off}} = 0.01\%$, the material behaviour can be better predicted by kinematic strain-hardening model, the plastic anisotropy of the deformed material is evident, the changes of anisotropy after deformation are considerable and cannot be disregarded.

For better illustration of the evolution of anisotropy, the experimental results will be shown as ellipses being sections of the yield surface made by the plane of non-vanishing stress components σ_x, τ_{xy} in the stress space. This graphical representation is based on the mixed isotropic-kinematic strain hardening model. Ellipses were reconstructed from two points corresponding to the yield limit in tension and compression assuming that (see Fig. 2):

- the ellipse axes ratio remains constant, $a/b = \text{const}$,
- the ellipse moves in the direction of σ_x axis, $\alpha_{xy} = 0$,
- the ellipse does not rotate, $\phi = 0$.

For comparison, ellipses corresponding to isotropic and kinematic strain-hardening models for materials with initial deformation will be shown in figures, together with the ellipse corresponding to the isotropic material in virgin state.

The ellipses for PA6 aluminium alloy determined for $\varepsilon_{\text{off}} = 0.01\%$ are shown in Fig. 16 and the ellipses corresponding to $\varepsilon_{\text{off}} = 1\%$ are shown in Fig. 17. It can

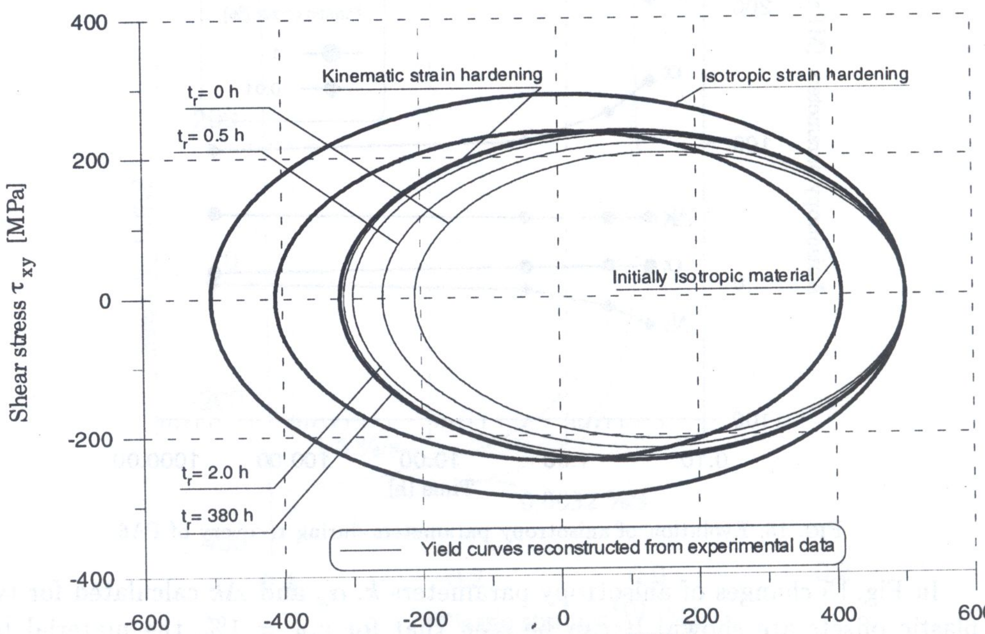

FIG. 16. Comparison of strain-hardening hypothesis with experimental data for PA6 alloy, plastic offset $\varepsilon_{\text{off}} = 0.01\%$.

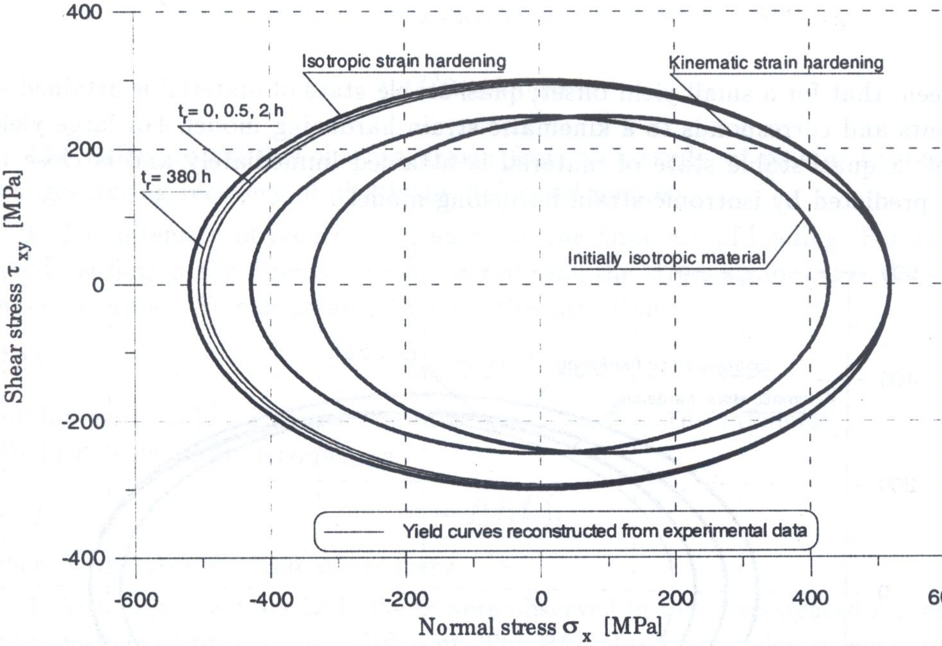

FIG. 17. Comparison of strain-hardening hypothesis with experimental data for PA6 alloy, plastic offset $\varepsilon_{\text{off}} = 1\%$.

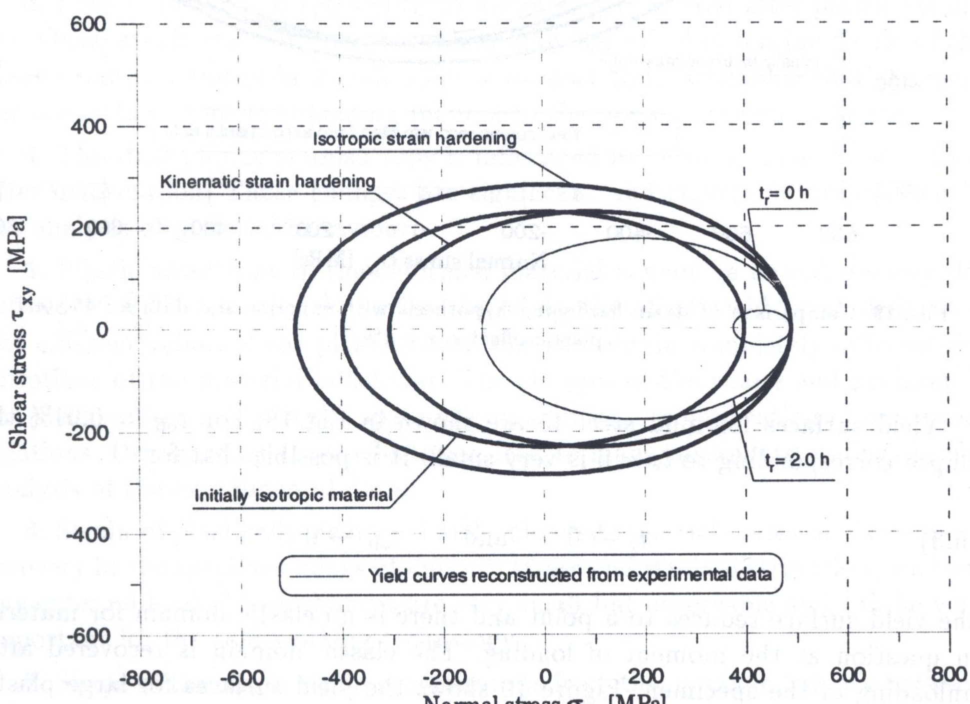

FIG. 18. Comparison of strain-hardening hypothesis with experimental data for 45 steel, plastic offset $\varepsilon_{\text{off}} = 0.01\%$.

be seen, that for a small yield offset, quasi-stable state of material is attained in 2 hours and corresponds to a kinematic strain-hardening model. For large yield offset, a quasi-stable state of material is attained immediately and is close to that predicted by isotropic strain-hardening model.

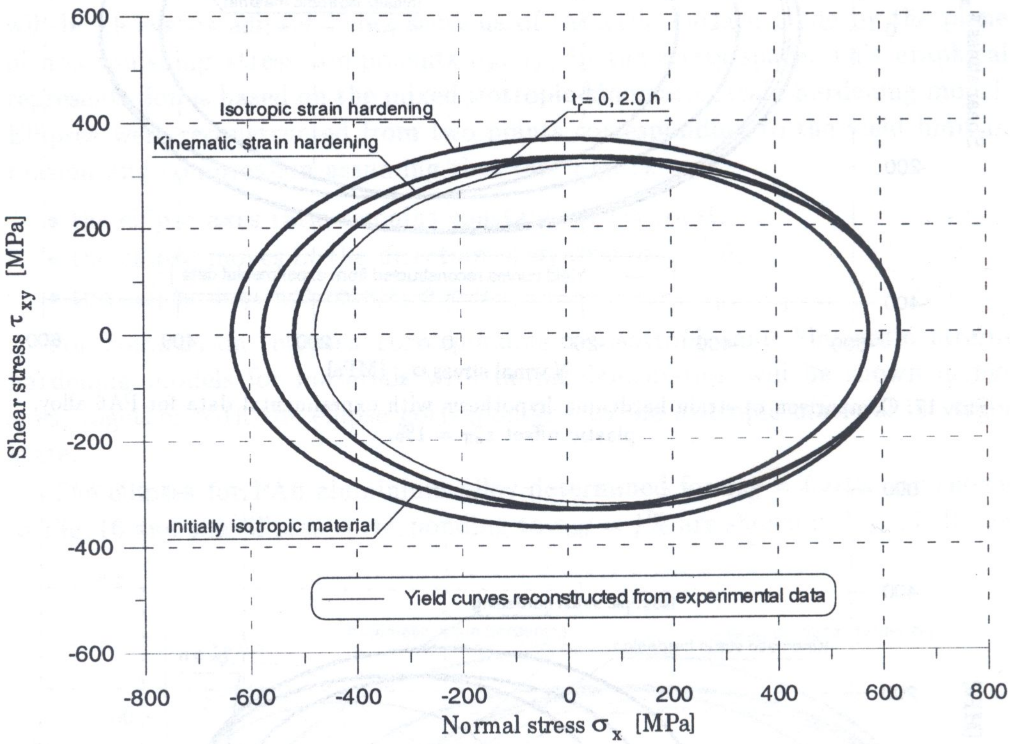

FIG. 19. Comparison of strain-hardening hypothesis with experimental data for 45 steel, plastic offset $\varepsilon_{\text{off}} = 1\%$.

Yield surfaces for mild steel 45 are shown in Fig. 18. For $\varepsilon_{\text{off}} = 0.01\%$ the ellipse corresponding to $t_r = 0$ is very small. It is possible that for

$$(6.3) \qquad t_r \to 0 \qquad \text{and} \qquad \varepsilon_{\text{off}} \to 0$$

the yield surface reduces to a point and there is no elastic domain for material in question at the moment of loading. The elastic domain is recovered after unloading of the specimen. Figure 19 shows the yield surfaces for large plastic offset. The surfaces corresponding to $t_r = 0$ and 2 hours coincide. The strain hardening is close to that predicted by the kinematic strain-hardening model and does not change in time.

7. Conclusions

The following conclusions are drawn from this study of plastic anisotropy changes during recovery of plastically deformed metals:

1. The intensity of recovery is related to the direction of loading. For subsequent loading in the direction of the initial one, the stress-strain curve does not change in time. We can assume that for this direction

$$\sigma = f(\varepsilon), \tag{7.1}$$

but for every other direction of subsequent loading the influence of recovery should be taken into account, i.e.

$$\sigma = f(\varepsilon, t_r), \tag{7.2}$$

where t_r denotes the time of recovery.

2. Although the described effects were observed in two investigated materials only, the rate of recovery was different. The PA6 aluminium alloy recovers much faster than mild steel 45.

3. Elastic domain for the deformed material is recovered after plastic straining. Quasi-stable state of PA6 aluminium alloy deformed in tension to 4% of the total strain is attained in 2 hours. For mild steel 45 it is possible that the yield surface at the moment of loading reduces to the point in the stress space.

4. The state of plastic anisotropy is influenced by recovery and varies in time after deformation. Those changes are significant and cannot be disregarded in the analysis of material behaviour.

5. Plastic anisotropy of the deformed material cannot be unambiguously described with the use of yield surface based on the offset yield point definition. For different values of the plastic offset, one can obtain completely different descriptions of the material behaviour. The changes of the shape and position of the yield surface in the stress space are an additional complication of our investigations. Disregarding those effects can lead to many misunderstandings in the analysis of the experimental data.

6. Strain of plastically deformed and unloaded material varies in time due to recovery in the specimen zones of uniform stress and strain distribution, without any external load. These changes are very small but observable and can be very important for the cold-working technology.

7. Shape of the stress-strain curves results from the dynamic balance between strain-hardening and recovery. This effect was observed as the difference in the shape of stress-strain loops for cyclic deformations of materials with different strain rates.

References

1. M.T. Huber, *Speçific strain energy as a measure of strength of materials* [in Polish], Czasopismo Techniczne, Lwów, pp. 663–698, 1904.
2. R. v. Mises, *Mechanik der plastischen Formänderung von Kristallen*, Zeitschr. Angew. Math. Mech., **8**, 3, pp. 161–185, 1928.
3. L. Shi and D.O. Northwood, *The mechanical behavior of an ANSI type 310 stainless steel*, Acta Metall. Mater., **43**, 2, pp. 453–460, 1995.
4. W. Szczepiński, *On deformation-induced plastic anisotropy of sheet metals*, Arch. Mech., **45**, 1, pp. 3–38, 1993.
5. G. Socha and W. Szczepiński, *On experimental determination of the coefficients of plastic anisotropy in sheet metals*, Arch. Mech., **46**, 1-2, pp. 177–190, 1994.
6. L. Dietrich, R. Kiryk, G. Socha and M. Śliwowski, *Identification of plastic anisotropy of aluminium alloys* [in Polish], IFTR Reports, 26/1994.
7. L. Dietrich, *Experimental determination of plastic anisotropy of metals* [in Polish], IFTR Reports, 33/1994.

POLISH ACADEMY OF SCIENCES
INSTITUTE OF FUNDAMENTAL TECHNOLOGICAL RESEARCH
e-mail: gsocha@ippt.gov.pl

Received August 14, 1996.